BIOCHEMISTRY

 Volume 43, Number 29 July 27, 2004

Articles

Homology Modeling of the Human Microsomal Glucose 6-Phosphate Transporter Explains the Mutations That Cause the Glycogen Storage Disease Type Ib†

Jonas Almqvist,‡ Yafei Huang,§ Sven Hovmöller,‡ and Da-Neng Wang*,§

Department of Structural Chemistry, Arrhenius Laboratory, Stockholm University, S-104 05 Stockholm, Sweden, and Skirball Institute of Biomolecular Medicine and Department of Cell Biology, New York University School of Medicine, 540 First Avenue, New York, New York 10016

Received April 5, 2004; Revised Manuscript Received May 26, 2004

ABSTRACT: Glycogen storage disease type Ib is caused by mutations in the glucose 6-phosphate transporter (G6PT) in the endoplasmic reticulum membrane in liver and kidney. Twenty-eight missense and two deletion mutations that cause the disease were previously shown to reduce or abolish the transporter's activity. However, the mechanisms by which these mutations impair transport remain unknown. On the basis of the recently determined crystal structure of its *Escherichia coli* homologue, the glycerol 3-phosphate transporter, we built a three-dimensional structural model of human G6PT by homology modeling. G6PT is proposed to consist of 12 transmembrane α-helices that are divided into N- and C-terminal domains, with the substrate-translocation pore located between the two domains and the substrate-binding site formed by R28 and K240 at the domain interface. The disease-causing mutations were found to occur at four types of positions: (I) in the substrate-translocation pore, (II) at the N-/C-terminal domain interface, (III) in the interior of the N- and C-terminal domains, and (IV) on the protein surface. Whereas class I mutations affect substrate binding directly, class II mutations, mostly involving changes in side chain size, charge, or both, hinder the conformational change required for substrate translocation. On the other hand, class III and class IV mutations, often introducing a charged residue into a helix bundle or at the protein−lipid interface, probably destabilize the protein. These results also suggest that G6PT operates by a similar antiport mechanism as its *E. coli* homologue, namely, the substrate binds at the N- and C-terminal domain interface and is then transported across the membrane via a rocker-switch type of movement of the two domains.

Glycogen storage disease type I (von Gierke's disease), a group of autosomal recessive disorders, is characterized by severe hepatomegaly, osteoporosis, enlarged kidneys, growth retardation, hypotonia with delayed acquisition of motor skills, platelet dysfunctions, and a tendency toward infections associated with neutropenia (*1*). The disorder is caused by a dysfunction in the glucose-6-phosphatase (G6Pase)[1] system in the endoplasmic reticulum (ER) in the liver and kidney (*2*, *3*). The ER takes up glucose 6-phosphate (G6P) by the G6P transporter (G6PT), and the imported sugar−phosphate molecule is hydrolyzed by the enzyme G6Pase into glucose and phosphate (P_i), which are then reexported back to the

† The work was partly funded by the National Institutes of Health (Grant DK RO1-53973). J.A. and S.H. were supported by the Swedish Research Council (VR).

* Corresponding author. Tel: 212-263-8634. Fax: 212-263-8951. E-mail: wang@saturn.med.nyu.edu.

‡ Stockholm University.

§ New York University School of Medicine.

10.1021/bi049334h CCC: $27.50
Published on Web 07/01/2004

cytoplasm (*4*). A deficiency of the G6Pase enzyme results in glycogen storage disease type Ia (GSD-Ia), whereas a defect in the G6P transporter causes glycogen storage disease type Ib (GSD-Ib). In the past few years, various mutations in the *G6PT* gene that cause GSD-Ib have been identified, including 28 missense, 2 codon deletion, 15 insertion/deletion, 10 nonsense, and 14 splicing mutations (*2*, *3*). Among them, the transport activities of the 28 missense and 2 deletion mutations have been characterized by microsomal transport assays (*3*, *5*). On the protein and mechanistic levels, however, the structural changes caused by these mutations are unknown, and consequently, the molecular pathogenesis of the GSD-Ib disease is poorly understood.

G6PT is a secondary transporter protein embedded in the ER membrane (*4*, *6*). The human protein consists of 429 amino acids (*7*). Using a marker peptide and proteolysis, Pan and co-workers showed that both the amino and carboxyl termini of the protein are in the cytoplasm (*8*). The transmembrane topology of the protein, however, is controversial: two topology models, one with 10 (*8*) and the other with 12 (*7*) transmembrane α-helices, have been proposed. Since no purification system is yet available for the human protein, direct biochemical and biophysical studies have not been possible. However, bacterial homologues of G6PT have been studied extensively. As a secondary membrane transporter, G6PT belongs to the organophosphate:phosphate antiporter (OPA) family of the major facilitator superfamily (MFS) (*9*). Bacterial members of the OPA family include the glucose 6-phosphate transporter (UhpT) and the glycerol 3-phosphate transporter (GlpT) (*10*). Both UhpT and GlpT from the *Escherichia coli* inner membrane have been overexpressed and purified and their transport activities measured in reconstituted proteoliposomes (*11*, *12*). Mutagenesis and functional studies on UhpT suggested certain residues that are located in the substrate-translocation pore or involved in substrate binding (*13*, *14*). Recently, the structure of GlpT from *E. coli* was determined to 3.3 Å resolution using X-ray crystallography (*15*, *16*). The structure revealed the substrate-translocation pathway and the substrate-binding site in the protein and suggested a mechanism for substrate transport. Since human G6PT shares significant sequence homology with its *E. coli* homologues, the structural and mechanistic information on the bacterial transporters should also shed light on the mechanism of the human protein.

With the recent successes in structural biology of membrane proteins from bacterial sources (*17*, *18*), homology modeling has been used to obtain 3D structural information for various mammalian membrane proteins, for which direct structural information is sparse. Models of G-protein-coupled receptors built using the rhodopsin structure as a template predicted the binding of various ligands (*19*). Homology modeling of inwardly rectified potassium channels based on the bacterial KcsA protein suggested a distorted ion selectivity filter for certain mutations, explaining their reduced conductance (*20*). For transporters, the 4.5 Å resolution structure of MsbA from *Vibrio cholera* (*21*) proteins has been used to model the human multidrug resistance proteins Pgp and MRP1 in the same ATP-binding cassette (ABC) transporter family, providing important mechanistic insight for these important drug-exporting proteins in tumor cells (*22*−*25*).

An understanding of the molecular mechanism underlining the GSD-Ib disorder requires detailed structural information on the G6PT protein. To this end, we have built a three-dimensional (3D) model of human G6PT using the crystal structure of its *E. coli* homologue GlpT as a template. The 28 missense and 2 deletion mutations that cause GSD-Ib were mapped onto the 3D G6PT model. Possible structural changes brought by these mutations and their effects on the substrate translocation were examined.

MATERIALS AND METHODS

Multiple Sequence Alignment. The amino acid sequence of human G6PT (O43826) was aligned with the following five OPA proteins that were found to have >23% sequence identity: G6PT from mouse (AAC79840), GlpT from *E. coli* (P08194), GlpT from *Bacillus subtilis* (P37948), UhpT from *E. coli* (P13408), and UhpT from *Salmonella typhimurium* (P27670). The protein sequences were retrieved from the Swiss-Prot/TrEMBL database and were compared using the program BLAST (*26*). The multiple sequence alignment was constructed using T-COFFEE (*27*). In the preliminary alignment, a total of six gaps were located in regions near the termini of helices 3, 5, 10, 11, and 12 in the corresponding GlpT structure template. These gaps were manually moved to the nearest loop regions in order to preserve the secondary structure between target and template (*28*), in agreement with the predicted transmembrane regions. In addition, the *E. coli* GlpT sequence was changed from the Swiss-Prot entry to account for the 8 unseen residues in the central loop of the crystal structure and mutations of L2G and of the last four residues at the C-terminus (RNGG → LVPR) that were required to produce the GlpT crystals (*12*, *15*).

Topology Prediction. We used several popular programs to predict the topology from its amino acid sequence for G6PT, using GlpT as a control. The programs were DAS (*29*), HMMTOP (*30*), MEMSAT (*31*), PHDhtm (*32*), TMHMM (*33*), TMpred (*34*), and TopPred (*35*). For HMMTOP, we also used the known sidedness of the N- and C-termini of the proteins relative to the membrane to improve the accuracy of the predictions (*36*).

Homology Model Building of the Three-Dimensional Structure. Using the above sequence alignment, three-dimensional models of human G6PT were built by homology modeling with the MODELLER software (*37*). The crystal structure of GlpT (*16*) was used as the structural template. Twelve sets of 100 homology models were generated, six sets with varying numbers of residues subjected to helical restraints and the others without. From each set, the five models with the lowest value of the MODELLER objective function were evaluated using VERIFY-3D (*38*), PROCHECK (*39*), and WHAT-IF (*40*). On the basis of these tests, the best performing model was selected as the final model. The

[1] Abbreviations: 3D, three dimensional; ABC, ATP-binding cassette; G3P, glycerol 3-phosphate; G6P, glucose 6-phosphate; G6Pase, glucose-6-phosphatase; G6PT, mammalian glucose 6-phosphate transporter; GlpT, bacterial glycerol 3-phosphate transporter; GSD-Ia, glycogen storage disease type Ia; GSD-Ib, glycogen storage disease type Ib; MFS, major facilitator superfamily; OPA, organophosphate:phosphate antiporter; P_i, inorganic phosphate; UhpT, bacterial glucose 6-phosphate transporter.

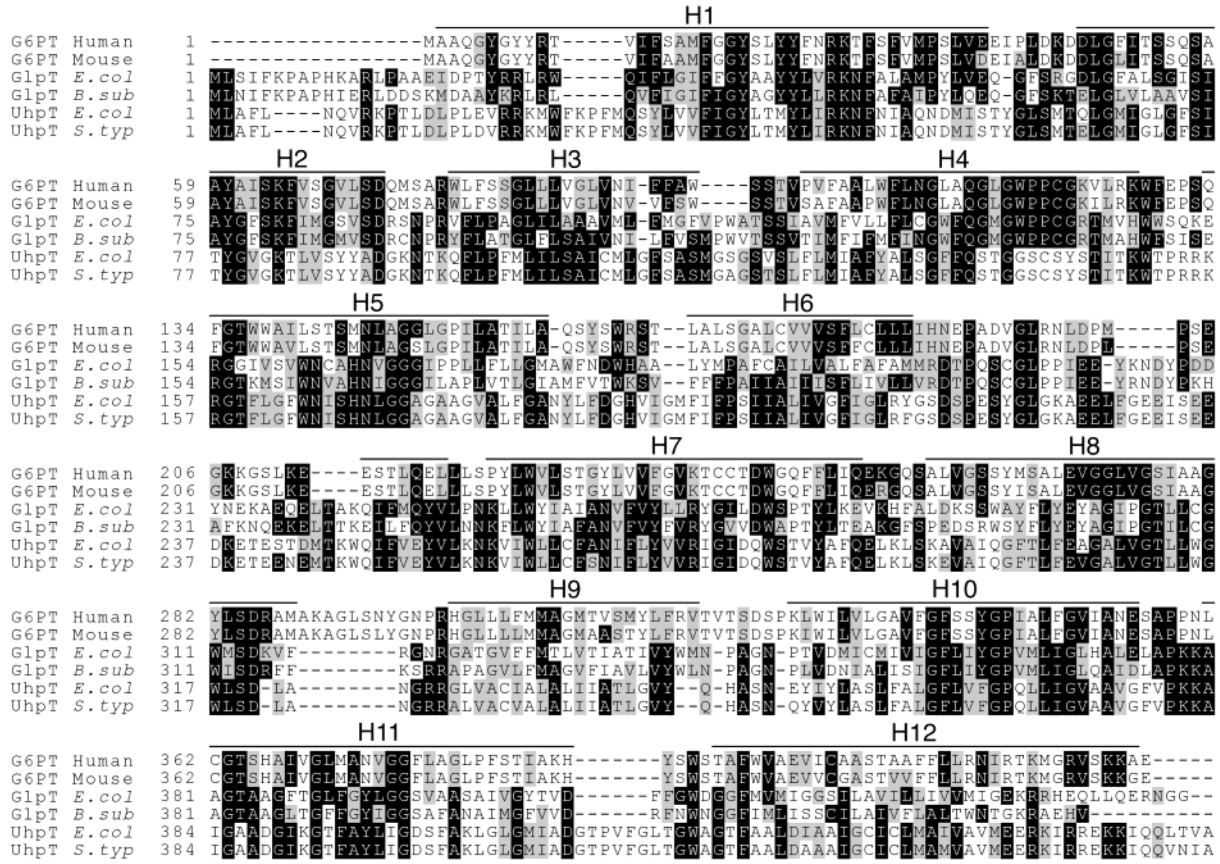

FIGURE 1: Multiple sequence alignment of human G6PT with other members of the OPA family. Residues conserved in at least half of the proteins are highlighted in black (identical matches) or gray (similar matches). The positions of the 12 transmembrane α-helices are indicated. *E.col* = *Escherichia coli*; *B.Sub* = *Bacillus subtilis*; *S.typ* = *Salmonella typhimurium.*

cavity volume within the protein model was calculated using the program VOIDOO (*41*). Finally, to investigate their structural changes and possible functional consequences, disease-causing missense and deletion mutations (*3*, *5*) were mapped onto the wild-type G6PT model using MODELLER.

RESULTS

Sequence Homology and Transmembrane Topology. The human glucose 6-phosphate transporter belongs to the OPA family of the major facilitator superfamily. Eukaryotic and prokaryotic members of the transporter family share significant amino acid sequence homology, and we therefore aligned the amino acid sequences of the G6PT proteins from human and mouse with those of their bacterial homologues UhpT and GlpT (Figure 1). The sequence identities among bacterial OPA proteins range from 30% to 60%, whereas the identities between bacterial and mammalian proteins are 20−30%. Except at the N-terminal region where the mammalian proteins are 15−18 amino acids longer, a reflection of the lack of a signal peptide for ER membrane proteins, the conserved residues distribute across the entire protein sequence. In particular, residues that are known to be critical for the configuration or packing of transmembrane α-helices, such as prolines and glycines (*42*, *43*), are well conserved among members of the OPA family (Figure 1). Human G6PT shares 27% amino acid sequence identity with its *E. coli* homologue, the GlpT protein, and their overall sequence similarity is 54%. A BLAST search between the two sequences generated a score of 129 with an *E* value of 8×10^{-29}, indicating strong similarity in their folds (*26*). For the questionable region between N27 and R77 in G6PT, corresponding to part of helix 1 and the entire helix 2 in the 12-helix model (*7*) but assigned as a long, single loop in the 10-helix model (*8*), the identity and similarity are as high as 45% and 63%, respectively. Importantly, proteins that are large and share sequence identities over 30% uniformly across the entire sequence almost always have the same fold (*44*−*47*).

We propose that G6PT adopts the same transmembrane topology as GlpT (*16*), with 12 transmembrane α-helices connected by loop regions (Figure 2). Besides the significant sequence identity discussed above, additional reasons are the following. First, secondary structure prediction favored a 12-helix transmembrane topology for G6PT. The DAS program predicted 11 helices for both G6PT and GlpT, whereas predictions by MEMSAT, PHDhtm, and TopPred yielded a 12-helix model for both proteins. The other three programs, HMMTOP, TMHMM, and TMPred, predicted 11 helices for G6PT and 12 helices for GlpT, respectively. However, when the cytoplasmic location of the N- and C-termini (*8*) was included in the predictions, HMMTOP also predicted 12 helices for GlpT as well as G6PT, in agreement with the results from MEMSAT, PHDhtm, and TopPred. It has been shown that the inclusion of even one experimental data point, say the C-terminal location, increased the accuracy of predictions for membrane proteins from 55% to 70% for all of the membrane proteins from three genomes (*36*), including *E. coli*. Thus, a 12-helix model for G6PT is more reasonable. Second, three known structures of MFS proteins, GlpT (*16*), the *E. coli* lactose permease (LacY) (*48*), and the oxalate

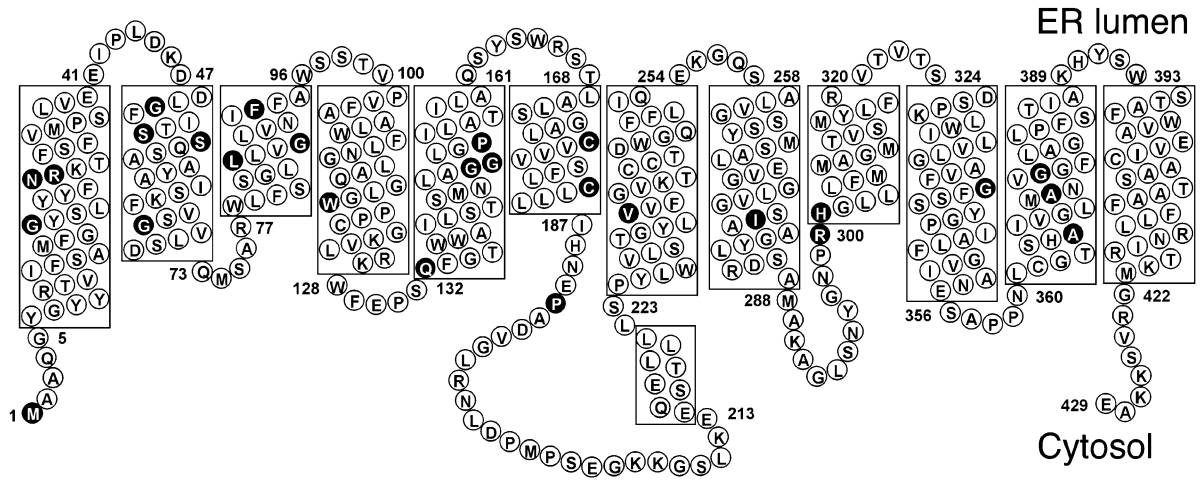

FIGURE 2: Proposed topology of G6PT with 12 transmembrane α-helices. Locations of GSD-Ib-causing mutations are indicated in black.

transporter (OxlT) from *Oxalobacter formigenes* (*49*, *50*), all have the same 12-transmembrane helix topology, even though their sequence identity is only 12−14%, while the sequence identity between G6PT and GlpT is much higher. The transmembrane helices were thereby designated H1 to H12 and the connecting loops L1−2 to L11−12. In addition to the differences in the H1−H2 region, helix 2 in the 10-helix model became H3 and was necessarily inverted, and the loop connecting helices 2 and 3 became H4 in the 12-helix model. The last eight helices in our model, H5 to H12 (Q133-M421), where the sequence identity between GlpT and G6PT is only 21%, correspond well with helices 3−10 (W137−L414) in the 10-helix model.

Overall Three-Dimensional Structure. On the basis of the above sequence alignment (Figure 1), homology modeling was carried out for the human G6PT protein using the crystal structure of its *E. coli* homologue GlpT (*16*) as a template. The best models with and without helical restraints were very similar. To avoid undue bias, we chose the best one derived without helical restraints as the final model. This G6PT model (Figure 3A) has adequate stereochemical properties. Ramachandran plot analysis showed that the backbone torsion angles are mostly in the favorable regions, whereas deviations of the bond lengths and angles from the mean standards were found to be reasonable, with root-mean-square deviations for bond length and angle of 0.019 Å and 2.2°, respectively. As expected, the G6PT structural model, to a large extent, resembles the GlpT structure (*16*). Briefly, the G6PT molecule is composed of an N-terminal half and the C-terminal half that are related by a central pseudo-2-fold symmetry axis perpendicular to the membrane plane. This pseudo-2-fold symmetry reflects the weak sequence homology between the two halves of the protein (at 19% identity), a common feature of all MFS proteins. Both the N- and C-termini are in the cytoplasm. Each half of the protein consists of six transmembrane α-helices that are connected by extramembrane loops. Due to an eight amino acid insertion relative to the GlpT sequence, the L8−9 loop is 13 amino acids long. Most of the other intradomain loops are only five amino acids long, leaving little freedom for relative movements of the helices within each domain. Helices in both the N- and C-terminal domains are densely packed, and there are few cavities in the domain interior. The interactions between the N- and C-terminal domains,

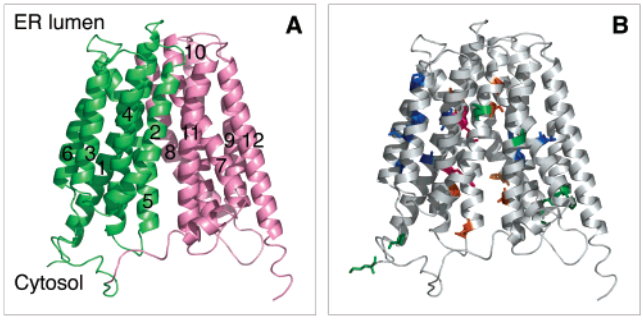

FIGURE 3: Ribbon diagrams of the structure model of human G6PT by homology modeling based on the crystal structure of its *E. coli* homologue GlpT, viewed from within the membrane. (A) Model for the wild-type G6PT. The N- and C-terminal domains are shown in green and purple, respectively. The 12 transmembrane α-helices are numbered by their order in the protein sequence. (B) Model of the wild-type G6PT shown together with the locations of 28 missense and 2 deletion mutations that cause glycogen storage disease type Ib. Affected residues are colored according to their position in the structure: pink, within the substrate-translocation pore; orange, at the N- and C-terminal domain interface; blue, in the interior of the N- or C-terminal domains; green, on the protein surface. This figure and Figure 4 were prepared using the program Pymol (*75*).

however, are relatively weak. The two domains are connected by a long, central loop L6−7, presumably flexible as in GlpT. While there are extensive van der Waals contacts between the domains at their interface, no salt bridges and few hydrogen bonds exist there. The convex curvature of the helices packed back to back at the domain interface suggests a rocker-switch type of movement between the two halves of the protein.

Proposed Substrate-Translocation Pathway and Substrate-Binding Site. Between the N- and C-terminal domains of G6PT is located a pore, open to the cytoplasm and closed off to the ER lumen, presumably representing the substrate-translocation pathway (Figures 3A and 4A). The structural model thus represents the cytoplasm-facing conformation of the transporter. The substrate-translocation pathway is lined by eight helices: H1, H2, H4, and H5, from the N-terminal half, and from their symmetry-related counterparts in the C-terminal domain, H7, H8, H10, and H11. The inner surface of the pore is mostly hydrophobic (data not shown), except

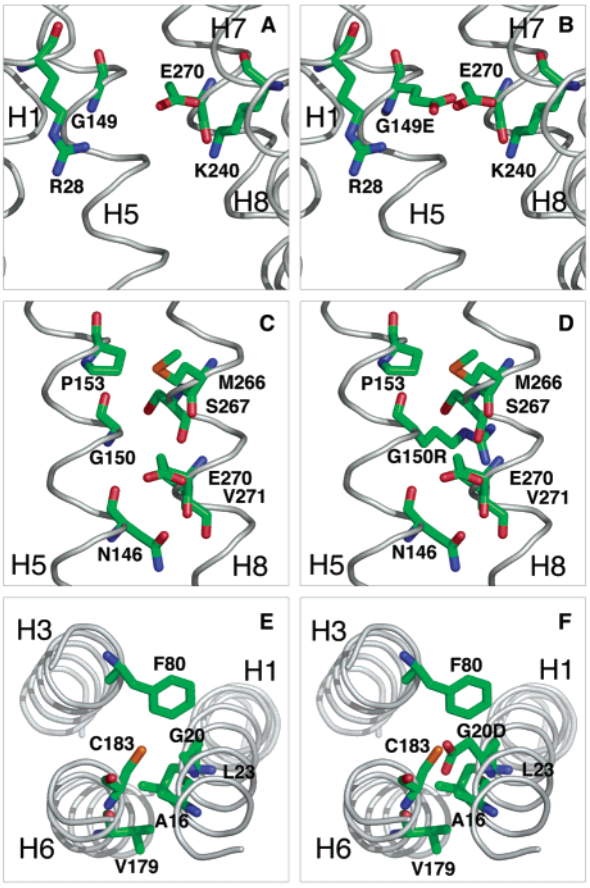

FIGURE 4: Examples of mutations of G6PT that disrupt the protein structure and thus diminish the transporter activity and cause glycogen storage disease type Ib. (A) Substrate-binding site in the wild-type protein. (B) Substrate-binding site with the G149E mutation. (C) H5−H8 interface in the wild-type protein. (D) H5−H8 interface with the G150R mutation. (E) Part of the N-terminal domain in the wild-type protein. (F) Part of N-terminal domain with the G20D mutation. Note the charge or the steric clashes introduced by each of the mutations. (A−D) are viewed from within the membrane, and (E, F) are viewed from the cytoplasm.

at the closed end of the pore in the middle of the membrane, where two positively charged residues, R28 from H1 and K240 from H7, are located. The closest distance between R28 and K240 is 10.1 Å. We propose that they form part of the substrate-binding site, similar to the substrate-binding site in the *E. coli* GlpT protein (*14*, *16*).

G6PT Mutations Were Divided into Four Classes. We mapped the 28 missense and 2 deletions that cause GSD-Ib (*6*) onto the 3D structural G6PT model (Figure 3B). These mutations occur at 26 positions in the wild-type protein (Figures 2 and 3B and Table 1). All of the mutations are in the helical regions, except M1V, P191L, R300H, and R300C, which are located in loops on the cytoplasmic side of the membrane (Figure 3B). On the basis of the position of these mutations, we categorized them into four classes (Table 1): class I, in the substrate translocation pore; class II, at the N-/C-terminal domain interface; class III, in the interior of the N- or C-terminal domains; class IV, at the protein's interface with the cytoplasm or with the lipid membrane. Each class of these mutations was analyzed separately as described below.

Class I: Mutations in the Substrate-Translocation Pore. A number of mutations were found in the proposed substrate-translocation pore (Figures 3B and 4A,B and Table 1). Notably, both R28H and R28C mutations occur on R28, one of the two positively charged residues proposed to be directly involved in substrate binding. The third mutation in this class, G149E, occurred at a position slightly on the lumenal side of the substrate-binding site, at a triangular plane with R28 and K240 (Figure 4B). Its distances to the key residues at the binding site are R28−G149, 9.5 Å, and K240−G149, 9.3 Å. Introduction of a negative charge near the binding site would probably change the positions of R28 and K240 as well as the positive electrostatic surface potential of the binding site and, therefore, affect the substrate binding. The last one in the category, W118R, is ∼7.0 Å to R28 from the cytoplasmic side. The location may be involved with binding to the glucose moiety of the substrate.

Class II: Mutations at the N-/C-Terminal Domain Interface. Several disease-causing mutations were found at the interface between the N-/C-terminal domains that is mostly formed by two pairs of curved helices, H2−H11 and H5−H8 (Figure 3B and Table 1). These single point mutations are G50R and S54R in H2, Q133P, G150R, and P153L in H5, I278N in H8, and A367T in H11 (*6*). Two of these mutations, Q133P and P153L, involve changes of a proline residue. The rest of the mutations change the size of the side chain at the interface or its charge or both. Four of the eight mutations in this class, G50R, S54R, G68R, and G150R, involve changing a neutral to a charged residue (Figure 4C,D), and two additional ones, I278N and A367T, change a hydrophobic residue to a hydrophilic one.

Class III: Mutations in the Interior of the N- and C-Terminal Domains. Twelve mutations that cause GSA-Ib were found to occur within the N- and C-terminal domains (Figure 3B and Table 1). Seven of them, G20D, N27K, G88D, C176R, C183R, G339D, and A373D, introduce a charged residue into the interior of the N- or C-terminal domains, often in the middle of a helix bundle. Four of the 12 mutations involve changing a glycine into a more bulky residue, G20D, G88D, G339D, and G339C (Figure 4E,F). Two deletion mutations that occur in a helix, ΔF93 in H3 and ΔV235 in H7, probably cause the neighboring residues to clash with its neighbors. In addition, because the Δ93 deletion occurs near the C-terminus of H3 which is followed by a short loop L3−4, the mutation may even affect the neighboring helix H4. Two other mutations involve a proline residue. L85P in H3 probably causes the helix to bend, whereas the H301P mutation probably disrupts H9.

Class IV: Mutations at the Protein's Interfaces with the Cytoplasm and with the Lipid Membrane. One mutation introducing a charged side chain, S55R, was found to be located at the protein−lipid interface (Figure 3B and Table 1). Two mutations, R300H and R300C, occur in L8−9 in the cytosol, which is part of the signature sequences for all members of the major facilitator superfamily (*51*). A mutation at the next residue in the protein sequence, H301P at the N-terminus of H9, may cause the helix to bend. Another mutation in this class abolishes G6PT's transport in a completely different manner: the M1V mutation causes the translation to start at M17 (*6*), resulting in a Δ1−16 truncation mutant lacking a substantial portion of H1. For the last mutation in the group, P191L, we were unable to suggest a reason for it to be lethal to the transporter's function.

Table 1: Mutations That Cause GSD-Ib and Their Possible Effects on the Protein Structure

mutation	location	activity (%)[a]	class[b]	comments
M1V	L1	0	IV	the M1V mutation causes the translation to start at M17, resulting in a Δ1−16 truncation mutant (*6*)
G20D	H1	0	III	G20 faces H6; mutation to an aspartate may affect the interface between H1 and H6
N27K	H1	0	III	N27 from H1 faces a region between H3, H4, and H6; a lysine in this region is too bulky and may cause clashes with the other three helices
R28C	H1	0	I	R28 is part of the substrate-binding site; a mutation may affect substrate binding directly
R28H	H1	0	I	see comments for R28C
G50R	H2	0	II	mutation to an arginine may cause problem at the H2−H11 interface
S54R	H2	0	II	mutation to an arginine may cause problem at the H2−H11 interface
S55R	H2	0	IV	S55 faces the lipids; mutation to a charged residue is unfavorable
G68R	H2	8.1	II	G68 is at the interface with H11; mutation to an arginine may cause problems at the N-/C-terminal domain interface in the outward-facing conformation
L85P	H3	0	III	L85 faces the lipids; mutation to a proline may cause a kink in the otherwise straight H3, causing the helix to bend toward H1 and H4
G88D	H3	2.2	III	G88 interacts with H6; mutation to an aspartate may disrupt the helix packing
ΔF93	H3	0	III	L3−4 is only 5 amino acids long; a deletion may cause problem to the two helices
W118R	H4	0	I	W118 faces the pore and is at the N/C interface; mutation to an arginine there may affect the pore closing in the outward-facing conformation; R118 may also affect the position of R28
Q133P	H5	0	II	mutation to a proline may change the curvature of H5
G149E	H5	0	I	G149 is in a triangular plane with R28 and K240, which are part of the proposed substrate-binding site; a G149E mutation introduces a negatively charged residue and may change the positive electrostatic surface potential there
G150R	H5	0	II	mutation may cause steric clashes with H8 at the N/C interface
P153L	H5	8.6	II	mutation may cause unfavorable interactions with H8 at the N/C interface
C176R	H6	0	III	an arginine causes clashes with side chains of H1 and H3
C183R	H6	0	III	C183 faces H1; mutation to an arginine may affect the interface between H1 and H6
P191L	L6−7	0	IV	
ΔV235	H7	0	III	deletion may destabilize H7
I278N	H8	10.4	II	mutation may cause steric clashes at the H5−H8 interface
R300C	L8−9	5.2	IV	R300 is the last residue in loop L8−9 and forms an ion pair with E355 of H10; loss of this interaction may affect the curvature of H8
R300H	L8−9	7.1	IV	R300 is the last residue in loop L8−9 and forms an ion pair with E355 of H10; loss of this interaction may affect the curvature of H8
H301P	H9	24.2	IV	mutation to a proline initiating this helix could bend the helix
G339C	H10	4.9	III	G339 is located at the interface with H8; mutation to a cysteine may cause steric clashes at the H8−H10 interface
G339D	H10	0	III	see comments for G339C
A367T	H11	23.1	II	mutation to a threonine may cause problem at the H2−H11 interface
A373D	H11	0	III	A373 faces H7; mutation to an aspartate may cause steric clashes and thereby destabilize the H11−H7 interface
G376S	H11	5.6	IV	G376 faces the lipid; it is part of a hydrophobic region in H11; energetically, it would be unfavorable to introduce a polar residue

[a] See ref *6*. [b] Class I, mutation within the substrate-translocation pore; class II, mutation at the N-/C-domain interface; class III, mutation in the interior of the N- or C-terminal domains; class IV, mutation on the protein surface.

DISCUSSION

The human glucose 6-phosphate transporter belongs to the organophosphate:phosphate antiporter family, one of the 38 transporter families identified in the major facilitator superfamily thus far (*9*). On the protein level, while members within a family are reasonably homologous, the sequence homology is rather low or undetectable between families within the superfamily. However, the available direct structural information on three MFS proteins (*16*, *48*−*50*) indicates that all proteins in the superfamily share the same topology and have very similar three-dimensional structures as well. This is even more significant considering the absence of significant sequence homology among the three proteins. The human G6PT and the *E. coli* GlpT proteins belong to the same OPA family and share 27% identity and 54% similarity in amino acid sequence. In addition, secondary structure predictions, when the experimentally determined C-terminal location was included in the input, also favored a 12-helix topology. We therefore assumed that the two proteins adopt very similar three-dimensional structures, which allowed us to justify building a structural model for human G6PT based on the GlpT crystal structure (Figures 2 and 3A). It follows that the two proteins may share similar substrate-translocation mechanisms.

The structural model of human G6PT that we obtained by homology modeling consists of an N- and a C-terminal domain related by a pseudo-2-fold symmetry (Figure 3A). Separated by a long, central loop, the two compact domains each contain six transmembrane α-helices that are connected by short, extramembrane loops. The substrate-binding site is believed to be located at the domain interface. The two pairs of long helices at the domain interface, H2−H11 and H5−H8, are highly curved, and they pack in a back-to-back manner like an hourglass. Obviously, this 12-helix structure is inconsistent with the 10-helix topology model of G6PT (*8*), which was largely based on data from protein glycosylation experiments. When point mutation T53N or S55N (in H2 of our model) was introduced, glycosylation of G6PT was detected (*8*). Such glycosylation was possible only if T53N and S55N were in the ER lumen, lending support to the 10-helix model. Importantly, however, these two glycosylated mutants were nonfunctional (*8*). Glycosylation of

membrane proteins is critical for their membrane targeting and folding (*52*, *53*); misglycosylation can cause misfolding (*54*−*56*). It is therefore possible that the two mutants were not properly folded in the ER membrane.

Our three-dimensional G6PT model, in combination with mutation data, provides information on the transporter's molecular mechanism. Two-thirds of the known mutations in G6PT (Figure 3B and Table 1) abolish the protein's substrate transport completely, with the remaining 10 showing activities of 2−25% of the wild type (*5*, *6*). These mutations probably affect the transporter's activity in three different ways, by modifying the substrate-binding site, by changing the N- and C-terminal domain interface, or by destabilizing the protein. This suggests that both the putative substrate-binding site and the N-/C-terminal domain interface are critical for the transporter's activity. Their importance can be best understood if the human G6PT protein is a G6P/inorganic phosphate antiporter, as suggested by mutation data on the proteins from patients with GSD types Ib and Ic (*57*), and if it works by a similar mechanism as the *E. coli* GlpT protein. In such a mechanism, the substrate binds at the N- and C-terminal domain interface in the transporter and is then transported across the membrane via a rocker-switch type of movement of the two domains (*16*). Such an antiport mechanism for G6PT would also explain the markedly enhanced G6P uptake of microsomes in the presence of G6Pase activity (*5*, *58*). As G6Pase hydrolyzes G6P into glucose and P_i, its activity lowers the G6P concentration in the ER lumen and, at the same time, increases the P_i concentration. As a result, the lacking of accumulation of G3P in the ER lumen and a steeper P_i gradient across the membrane as the driving force facilitate the G6P−P_i exchange (*16*). This is in contrast to the uptake of G3P and G6P in *E. coli* by GlpT or UhpT, where multiple pathways of utilizing the organic phosphates are present but not a homologue of human G6Pase (*59*). Finally, the nondisease-causing mutation due to G6PT polymorphism (*57*, *60*), N198I, occurs in L6−7, the long central loop whose amino acid sequence is known to be unimportant for the function of MFS proteins (*61*).

Understandably, mutations in the proposed substrate-translocation pore (class I) can affect substrate binding directly (Figures 3B and 4A,B and Table 1). It was shown previously that these mutants express at similar levels as the wild-type G6PT (*5*, *6*). The loss of transport activity, therefore, is due to impaired protein activity, rather than reduction in expression levels. Like its bacterial homologues (*12*), the substrate binding in G6PT is expected to be via the negatively charged phosphate moiety of a substrate. The positive electrostatic surface potential around the binding site is therefore important. R28H, R28C, and G149E occur at the proposed substrate-binding site. They are likely to change the electrostatic surface potential there. Interestingly, "back-mutation" experiments carried out with UhpT, the G6P transporter from *E. coli*, on the equivalent residues at the substrate-binding site (*62*) agree with our model. Among the 14 arginines in UhpT, only the two equivalent to R28 and K240 of G6PT were found to be essential for UhpT's activity. The last residue in the category, W118, may be involved with binding to the glucose moiety of the substrate. A mutation to an arginine residue may therefore affect this binding. It is noted that the indole ring of W151 in the lactose-transporting LacY is a major part of the substrate-binding site by hydrophobic interactions (*48*).

Mutations at the N- and C-terminal domain interface in G6PT (class II) affect the side chain size or charge or the curvature of the helices (Figures 3B and 4C,D and Table 1). Seven of the 28 known missense mutations that cause GSD-Ib belong to this class. Having curved helices packed back to back at the domain interface is a common feature in all the three known structures of MFS proteins (*16*, *48*, *49*). As in GlpT, the curvature of H2, H5, H8, and H11 in G6PT is believed to be critical for the rocker-switch type of movement of the two domains associated with substrate translocation (*16*). The two mutations involving a proline residue (Q133P and P153L) are likely to change the helix curvature (*42*, *63*) and thus affect the conformational change. On the other hand, a change in residue charge or side chain size at the domain interface in G6PT can also hinder the relative movement of the two domains (Table 1).

Mutations of G6PT in the interior of the N- and C-terminal domains (class III) and at the interface with the lipids or cytoplasm (class IV) probably affect the protein's stability (Figures 3B and 4E,F and Table 1). Most of them introduce a charged residue in the middle of a helix bundle or at the protein−lipid interface. These changes are likely to destabilize the protein. Mutations from glycine into a more bulky residue may disrupt helix−helix packing, as glycine residues in membrane proteins are known to often be involved in helix−helix packing by forming weak C_α- - -H···O hydrogen bonds (*64*). The H301P mutation, as the first residue of H9, probably disrupts or even breaks the helix (*65*). On the cytosolic side of the molecule, R300C and R300H occur within one of the two MFS signature sequences (*9*, *51*), RXXXR in L2−3 and RXXR in L8−9 (Figure 2), which are known to be important for the protein's transport activity (*66*−*68*). These positively charged residues probably help to position and orient the transmembrane helices when the protein undergoes membrane insertion, as has been observed for the human erythrocyte glucose transporter (Glut1) (*69*). Interestingly, the change of the Glut1 equivalent of R300 in G6PT to a tryptophan residue (RXXXW) causes human Glut1 deficiency syndrome (*70*).

The above hypothesis on the stability of G6PT mutants agrees with the available experimental data on G6PT. In vitro transcription-translation assays showed that wild-type, R28H, G20D, ΔF93, and I278N constructs directed the synthesis of similar amounts of G6PT proteins (*71*). Therefore, the observed decrease in the synthesis of G20D, ΔF93, and I278N mutants may result from misfolding or rapid degradation of the mutant proteins in the cell. Recently, mutations in membrane proteins that destabilize the protein structure have attracted considerable attention (*72*). As has been shown with the multiple-spanning integral membrane protein diacylglycerol kinase of *E. coli*, destabilizing mutations often promote membrane protein misfolding (*73*). Sanders and Myers have argued that a 1.5 kcal/mol change in kinetic energy barriers, well within the range of free energy perturbations by a single amino acid mutation (*74*), is sufficient to reduce the membrane protein's folding efficiency by 10% at body temperature (*72*). Therefore, misfolding and misassembly of membrane proteins may be a common mechanism of causing human diseases.

ACKNOWLEDGMENT

We thank Drs. J. Y. Chou of NICHHD/NIH and P. C. Maloney of Johns Hopkins University School of Medicine for helpful discussions.

REFERENCES

1. McKusick, V. A. (1998) *Mendelian Inheritance in Man: A Catalog of Human Genes and Genetic Disorders*, Vol. 3, 12th ed., Johns Hopkins University Press, Baltimore, MD.
2. Janecke, A. R., Mayatepek, E., and Utermann, G. (2001) Molecular genetics of type 1 glycogen storage disease, *Mol. Genet. Metab. 73*, 117−125.
3. Chou, J. Y., Matern, D., Mansfield, B. C., and Chen, Y. T. (2002) Type I glycogen storage diseases: disorders of the glucose-6-phosphatase complex, *Curr. Mol. Med. 2*, 121−143.
4. Foster, J. D., and Nordlie, R. C. (2002) The biochemistry and molecular biology of the glucose-6-phosphatase system, *Exp. Biol. Med. 227*, 601−608.
5. Hiraiwa, H., Pan, C. J., Lin, B., Moses, S. W., and Chou, J. Y. (1999) Inactivation of the glucose 6-phosphate transporter causes glycogen storage disease type 1b, *J. Biol. Chem. 274*, 5532−5536.
6. Chen, L. Y., Pan, C. J., Shieh, J. J., and Chou, J. Y. (2002) Structure−function analysis of the glucose-6-phosphate transporter deficient in glycogen storage disease type Ib, *Hum. Mol. Genet. 11*, 3199−3207.
7. Gerin, I., Veiga-da-Cunha, M., Achouri, Y., Collet, J. F., and Van Schaftingen, E. (1997) Sequence of a putative glucose 6-phosphate translocase, mutated in glycogen storage disease type Ib, *FEBS Lett. 419*, 235−238.
8. Pan, C. J., Lin, B., and Chou, J. Y. (1999) Transmembrane topology of human glucose 6-phosphate transporter, *J. Biol. Chem. 274*, 13865−13869.
9. Pao, S. S., Paulsen, I. T., and Saier, M. H., Jr. (1998) Major facilitator superfamily, *Microbiol. Mol. Biol. Rev. 62*, 1−34.
10. Maloney, P. C., Ambudkar, S. V., Anatharam, V., Sonna, L. A., and Varadhachary, A. (1990) Anion-exchange mechanisms in bacteria, *Microbiol. Rev. 54*, 1−17.
11. Fann, M. C., and Maloney, P. C. (1998) Functional symmetry of UhpT, the sugar phosphate transporter of *Escherichia coli*, *J Biol. Chem. 273*, 33735−33740.
12. Auer, M., Kim, M. J., Lemieux, M. J., Villa, A., Song, J., Li, X. D., and Wang, D. N. (2001) High-yield expression and functional analysis of *Escherichia coli* glycerol-3-phosphate transporter, *Biochemistry 40*, 6628−6635.
13. Matos, M., Fann, M. C., Yan, R. T., and Maloney, P. C. (1996) Enzymatic and biochemical probes of residues external to the translocation pathway of UhpT, the sugar phosphate carrier of *Escherichia coli*, *J. Biol. Chem. 271*, 18571−18575.
14. Fann, M. C., Davies, A. H., Varadhachary, A., Kuroda, T., Sevier, C., Tsuchiya, T., and Maloney, P. C. (1998) Identification of two essential arginine residues in UhpT, the sugar phosphate antiporter of *Escherichia coli*, *J. Membr. Biol. 164*, 187−195.
15. Lemieux, M. J., Song, J., Kim, M. J., Huang, Y., Villa, A., Auer, M., Li, X. D., and Wang, D. N. (2003) Three-dimensional crystallization of the *Escherichia coli* glycerol-3-phosphate transporter: a member of the major facilitator superfamily, *Protein Sci. 12*, 2748−2756.
16. Huang, Y., Lemieux, M. J., Song, J., Auer, M., and Wang, D. N. (2003) Structure and mechanism of the glycerol-3-phosphate transporter from *Escherichia coli*, *Science 301*, 616−620.
17. Locher, K. P., Bass, R. B., and Rees, D. C. (2003) Structural biology. Breaching the barrier, *Science 301*, 603−604.
18. Harrison, S. C. (2004) Whither structural biology?, *Nat. Struct. Mol. Biol. 11*, 12−15.
19. Bissantz, C., Bernard, P., Hibert, M., and Rognan, D. (2003) Protein-based virtual screening of chemical databases. II. Are homology models of G-Protein Coupled Receptors suitable targets? *Proteins 50*, 5−25.
20. Capener, C. E., Proks, P., Ashcroft, F. M., and Sansom, M. S. (2003) Filter flexibility in a mammalian K channel: models and simulations of Kir6.2 mutants, *Biophys. J. 84*, 2345−2356.
21. Chang, G., and Roth, C. B. (2001) Structure of MsbA from *E. coli*: a homolog of the multidrug resistance ATP binding cassette (ABC) transporters, *Science 293*, 1793−1800.
22. Stenham, D. R., Campbell, J. D., Sansom, M. S., Higgins, C. F., Kerr, I. D., and Linton, K. J. (2003) An atomic detail model for the human ATP binding cassette transporter P-glycoprotein derived from disulfide cross-linking and homology modeling, *FASEB J. 17*, 2287−2289.
23. Campbell, J. D., Koike, K., Moreau, C., Sansom, M. S., Deeley, R. G., and Cole, S. P. (2004) Molecular modeling correctly predicts the functional importance of Phe594 in transmembrane helix 11 of the multidrug resistance protein, MRP1 (ABCC1), *J. Biol. Chem. 279*, 463−468.
24. Campbell, J. D., Biggin, P. C., Baaden, M., and Sansom, M. S. (2003) Extending the structure of an ABC transporter to atomic resolution: modeling and simulation studies of MsbA, *Biochemistry 42*, 3666−3673.
25. Seigneuret, M., and Garnier-Suillerot, A. (2003) A structural model for the open conformation of the mdr1 P-glycoprotein based on the MsbA crystal structure, *J. Biol. Chem. 278*, 30115−30124.
26. Altschul, S. F., Madden, T. L., Schaffer, A. A., Zhang, J., Zhang, Z., Miller, W., and Lipman, D. J. (1997) Gapped BLAST and PSI−BLAST: a new generation of protein database search programs, *Nucleic Acids Res. 25*, 3389−3402.
27. Notredame, C., Higgins, D. G., and Heringa, J. (2000) T-COFFEE: A novel method for fast and accurate multiple sequence alignment, *J. Mol. Biol. 302*, 205−217.
28. Bur, D., Dale, G. E., and Oefner, C. (2001) A three-dimensional model of endothelin-converting enzyme (ECE) based on the X-ray structure of neutral endopeptidase 24.11 (NEP), *Protein Eng. 14*, 337−341.
29. Cserzo, M., Wallin, E., Simon, I., von Heijne, G., and Elofsson, A. (1997) Prediction of transmembrane α-helices in prokaryotic membrane proteins: the dense alignment surface method, *Protein Eng. 10*, 673−676.
30. Tusnady, G. E., and Simon, I. (1998) Principles governing amino acid composition of integral membrane proteins: application to topology prediction, *J. Mol. Biol. 283*, 489−506.
31. Jones, D. T., Taylor, W. R., and Thornton, J. M. (1994) A model recognition approach to the prediction of all-helical membrane protein structure and topology, *Biochemistry 33*, 3038−3049.
32. Rost, B., Casadio, R., Fariselli, P., and Sander, C. (1995) Transmembrane helices predicted at 95% accuracy, *Protein Sci. 4*, 521−533.
33. Krogh, A., Larsson, B., von Heijne, G., and Sonnhammer, E. L. (2001) Predicting transmembrane protein topology with a hidden Markov model: application to complete genomes, *J. Mol. Biol. 305*, 567−580.
34. Hofmann, K., and Stoffel, W. (1993) TMbase—a database of membrane spanning proteins segments, *Biol. Chem. Hoppe-Seyler 374*, 166−171.
35. Claros, M. G., and von Heijne, G. (1994) TopPred II: an improved software for membrane protein structure predictions, *Comput. Appl. Biosci. 10*, 685−686.
36. Melen, K., Krogh, A., and von Heijne, G. (2003) Reliability measures for membrane protein topology prediction algorithms, *J. Mol. Biol. 327*, 735−744.
37. Sali, A., and Blundell, T. L. (1993) Comparative protein modelling by satisfaction of spatial restraints, *J. Mol. Biol. 234*, 779−815.
38. Luthy, R., Bowie, J. U., and Eisenberg, D. (1992) Assessment of protein models with three-dimensional profiles, *Nature 356*, 83−85.
39. Laskowski, R. A., MacArthur, M. W., Moss, D. S., and Thornton, J. M. (1993) PROCHECK: a program to check the stereochemical quality of protein structures, *J. Appl. Crystallogr. 26*, 283−291.
40. Rodriguez, R., Chinea, G., Lopez, N., Pons, T., and Vriend, G. (1998) Homology modeling, model and software evaluation: three related resources, *Bioinformatics 14*, 523−528.
41. Kleywegt, G. J., and Jones, T. A. (1994) Detection, delineation, measurement and display of cavities in macromolecular structures, *Acta Crystallogr. D50*, 178−185.
42. Williams, K. A., and Deber, C. M. (1991) Proline residues in transmembrane helices: structural or dynamic role? *Biochemistry 30*, 8919−8923.
43. Liu, Y., Engelman, D. M., and Gerstein, M. (2002) Genomic analysis of membrane protein families: abundance and conserved motifs, *Genome Biol. 3*, 1−12.
44. Chothia, C., and Lesk, A. M. (1986) The relation between the divergence of sequence and structure in proteins, *EMBO J. 5*, 823−826.
45. Sander, C., and Schneider, R. (1991) Database of homology-derived protein structures and the structural meaning of sequence alignment, *Proteins 9*, 56−68.

46. Flores, T. P., Orengo, C. A., Moss, D. S., and Thornton, J. M. (1993) Comparison of conformational characteristics in structurally similar protein pairs, *Protein Sci. 2*, 1811−1826.
47. Orengo, C. A., Michie, A. D., Jones, S., Jones, D. T., Swindells, M. B., and Thornton, J. M. (1997) CATH−a hierarchic classification of protein domain structures, *Structure 5*, 1093−1108.
48. Abramson, J., Smirnova, I., Kasho, V., Verner, G., Kaback, H. R., and Iwata, S. (2003) Structure and mechanism of the lactose permease of *Escherichia coli*, *Science 301*, 610−615.
49. Hirai, T., Heymann, J. A., Shi, D., Sarker, R., Maloney, P. C., and Subramaniam, S. (2002) Three-dimensional structure of a bacterial oxalate transporter, *Nat. Struct. Biol. 9*, 597−600.
50. Hirai, T., Heymann, J. A., Maloney, P. C., and Subramaniam, S. (2003) Structural model for 12-helix transporters belonging to the major facilitator superfamily, *J. Bacteriol. 185*, 1712−1718.
51. Maiden, M. C., Davis, E. O., Baldwin, S. A., Moore, D. C., and Henderson, P. J. (1987) Mammalian and bacterial sugar transport proteins are homologous, *Nature 325*, 641−643.
52. Parodi, A. J. (2000) Protein glucosylation and its role in protein folding, *Annu. Rev. Biochem. 69*, 69−93.
53. Goder, V., and Spiess, M. (2001) Topogenesis of membrane proteins: determinants and dynamics, *FEBS Lett. 504*, 87−93.
54. Hirschberg, C. B., Robbins, P. W., and Abeijon, C. (1998) Transporters of nucleotide sugars, ATP, and nucleotide sulfate in the endoplasmic reticulum and Golgi apparatus, *Annu. Rev. Biochem. 67*, 49−69.
55. d'Addio, M., Pizzigoni, A., Bassi, M. T., Baschirotto, C., Valetti, C., Incerti, B., Clementi, M., De Luca, M., Ballabio, A., and Schiaffino, M. V. (2000) Defective intracellular transport and processing of OA1 is a major cause of ocular albinism type 1, *Hum. Mol. Genet. 9*, 3011−3018.
56. Farinha, C. M., Nogueira, P., Mendes, F., Penque, D., and Amaral, M. D. (2002) The human DnaJ homologue (Hdj)-1/heat-shock protein (Hsp) 40 co-chaperone is required for the in vivo stabilization of the cystic fibrosis transmembrane conductance regulator by Hsp70, *Biochem. J. 366*, 797−806.
57. Veiga-da-Cunha, M., Gerin, I., Chen, Y. T., de Barsy, T., de Lonlay, P., Dionisi-Vici, C., Fenske, C. D., Lee, P. J., Leonard, J. V., Maire, I., McConkie-Rosell, A., Schweitzer, S., Vikkula, M., and Van Schaftingen, E. (1998) A gene on chromosome 11q23 coding for a putative glucose-6-phosphate translocase is mutated in glycogen-storage disease types Ib and Ic, *Am. J. Hum. Genet. 63*, 976−983.
58. Lei, K. J., Chen, H., Pan, C. J., Ward, J. M., Mosinger, B., Jr., Lee, E. J., Westphal, H., Mansfield, B. C., and Chou, J. Y. (1996) Glucose-6-phosphatase dependent substrate transport in the glycogen storage disease type-1a mouse, *Nat. Genet. 13*, 203−209.
59. Lin, E. C. C. (1996) Dissimilatory pathways for sugars, polyols and carboxylates, in *Escheriachia coli and Salmonella: Cellular and Molecular Biology* (Neidhardt, F. C., Curtiss, R. I., Ingraham, J. L., Lin, E. C. C., Low, K. B., Magasanik, B., Reznikoff, W. S., Riley, M., Schaechter, M., and Umbarger, H. E., Eds.) pp 307−342, ASM Press, Washington, DC.
60. Veiga-da-Cunha, M., Gerin, I., Chen, Y. T., Lee, P. J., Leonard, J. V., Maire, I., Wendel, U., Vikkula, M., and Van Schaftingen, E. (1999) The putative glucose 6-phosphate translocase gene is mutated in essentially all cases of glycogen storage disease type I non-a, *Eur. J. Hum. Genet. 7*, 717−723.
61. Hruz, P. W., and Mueckler, M. M. (2001) Structural analysis of the GLUT1 facilitative glucose transporter, *Mol. Membr. Biol. 18*, 183−193.
62. Fann, M., Davies, A. H., Varadhachary, A., Kuroda, T., Sevier, C., Tsuchiya, T., and Maloney, P. C. (1998) Identification of two essential arginine residues in UhpT, the sugar phosphate antiporter of *Escherichia coli*, *J. Membr. Biol. 164*, 187−195.
63. Yohannan, S., Faham, S., Yang, D., Whitelegge, J. P., and Bowie, J. U. (2004) The evolution of transmembrane helix kinks and the structural diversity of G protein-coupled receptors, *Proc. Natl. Acad. Sci. U.S.A. 101*, 959−963.
64. Senes, A., Ubarretxena-Belandia, I., and Engelman, D. M. (2001) The Cα- - -H···O hydrogen bond: a determinant of stability and specificity in transmembrane helix interactions, *Proc. Natl. Acad. Sci. U.S.A. 98*, 9056−9061.
65. Nilsson, I., Saaf, A., Whitley, P., Gafvelin, G., Waller, C., and von Heijne, G. (1998) Proline-induced disruption of a transmembrane α-helix in its natural environment, *J. Mol. Biol. 284*, 1165−1175.
66. Yamaguchi, A., Someya, Y., and Sawai, T. (1992) Metal-tetracycline/H+ antiporter of *Escherichia coli* encoded by transposon Tn10. The role of a conserved sequence motif, GXXXXRX-GRR, in a putative cytoplasmic loop between helices 2 and 3, *J. Biol. Chem. 267*, 19155−19162.
67. Yamaguchi, A., Kimura, T., Someya, Y., and Sawai, T. (1993) Metal-tetracycline/H+ antiporter of *Escherichia coli* encoded by transposon Tn10. The structural resemblance and functional difference in the role of the duplicated sequence motif between hydrophobic segments 2 and 3 and segments 8 and 9, *J. Biol. Chem. 268*, 6496−6504.
68. Jessen-Marshall, A. E., Paul, N. J., and Brooker, R. J. (1995) The conserved motif, GXXX(D/E)(R/K)XG[X](R/K)(R/K), in hydrophilic loop 2/3 of the lactose permease, *J. Biol. Chem. 270*, 16251−16257.
69. Sato, M., and Mueckler, M. (1999) A conserved amino acid motif (R-X-G-R-R) in the Glut1 glucose transporter is an important determinant of membrane topology, *J. Biol. Chem. 274*, 24721−24725.
70. Wang, D., Kranz-Eble, P., and De Vivo, D. C. (2000) Mutational analysis of GLUT1 (SLC2A1) in glut-1 deficiency syndrome, *Hum. Mutat. 16*, 224−231.
71. Chen, L. Y., Lin, B., Pan, C. J., Hiraiwa, H., and Chou, J. Y. (2000) Structural requirements for the stability and microsomal transport activity of the human glucose 6-phosphate transporter, *J. Biol. Chem. 275*, 34280−34286.
72. Sanders, C. R., and Myers, J. K. (2004) Disease-related misassembly of membrane proteins, *Annu. Rev. Biophys. Biomol. Struct. 33*, 25−51.
73. Nagy, J. K., and Sanders, C. R. (2004) Destabilizing mutations promote membrane protein misfolding, *Biochemistry 43*, 19−25.
74. Guerois, R., Nielsen, J. E., and Serrano, L. (2002) Predicting changes in the stability of proteins and protein complexes: a study of more than 1000 mutations, *J. Mol. Biol. 320*, 369−387.
75. DeLano, W. L. (2002) *The PyMOL User's Manual*, DeLano Scientific, San Carlos, CA.

BI049334H